

AD-A090 416

WHITE SANDS MISSILE RANGE NM INSTRUMENTATION DIRECTORATE
FINDING EDGES IN NOISY SCENES. (U)
JUN 80 R MACHUCA, A L GILBERT

F/6 5/8

UNCLASSIFIED

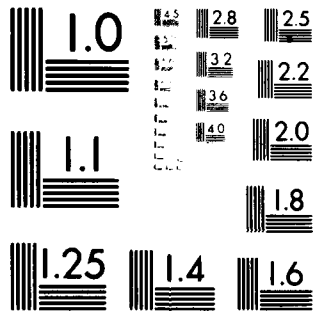
NL

[OF]

AD
AD-90 416



END
DATE
FILMED
11-80
DTIC



MICROCOPY RESOLUTION TEST CHART

NATIONAL BUREAU OF STANDARDS-1963-A

*MACHUCA & GILBERT

LEVEL

AD A090416

FINDING EDGES IN NOISY SCENES

PAUL MACHUCA, PhD.

ALTON L. GILBERT, PhD.

INSTRUMENTATION DIRECTORATE

WHITE SANDS MISSILE RANGE, NEW MEXICO 88002

JUN 80

Research into methods of identifying edges in a noisy scene has been an active field of investigation for many years. Treatment of the subject may be found in many books written over the past decade ([1], [2], and [3]) and many different approaches are proposed. Recently a survey and comparative analysis of the methods was made [7].

The body of this paper is segmented into 4 parts. In the first we derive and define a "Moment Operator" which we show to work well for step and ramp edges. Then, we define and characterize second order edges using the concept of the rotation of a point in a vector field and develop the detector analytically. In Section 3 we develop the algorithms for implementing the previously defined operators. Finally, in Section 4, these algorithms are evaluated using ROC curves and compared with previously known techniques.

The detection of edges to isolate objects in a scene is motivated by many distinct problems. One such problem arises in a tracking system where the input video image is analyzed and the object to be tracked identified. Subsequent input and feedback to the drive controls causes the sensor to re-orient to a new position in an attempt to maintain the same x-y coordinate position for the object in the field of view. While this problem motivated the research that led to this paper, the results herein discussed are much broader in scope and application. The constraints imposed by this problem led to a method that is useful in high data throughput systems.

DDC FILE COPY

DTIC
ELECTRA

OCT 16 1980

This document has been approved
for public release and sale; its
distribution is unlimited.

427

184230

80 10 16 029

455

SECTION 1. EDGES FROM MOMENTS

First order edge detection methods work in the following way: A picture function $f(x,y)$ is transformed to another picture function $F(x,y) = Tf(x,y)$ in such a way that the edges of objects in the scene will be in the set $\{(x,y): F(x,y) \geq W\}$ for some W . The usual method is to transform the picture using T equal to the gradient operator. Different edge detection methods correspond to different numerical approximations to the gradient.

The method used in our edge detection program is not based on derivatives. To reduce the effect of noise, this edge detection method uses integrals.

The reasoning for the use of moments to find edges is as follows. A digitized picture can be thought as a lamina whose density at each point is $f(x,y)$, so points of high intensity correspond to points of high density. A point (a,b) on an edge in the original function (see Figure 1) would correspond to a point in this lamina (digitized picture) with high densities on one side and lower densities on the other side. Thus if we look at a small lamina centered at point (a,b) and compute the center of mass of this small lamina, we can expect the center of mass to lie within an area of high densities.




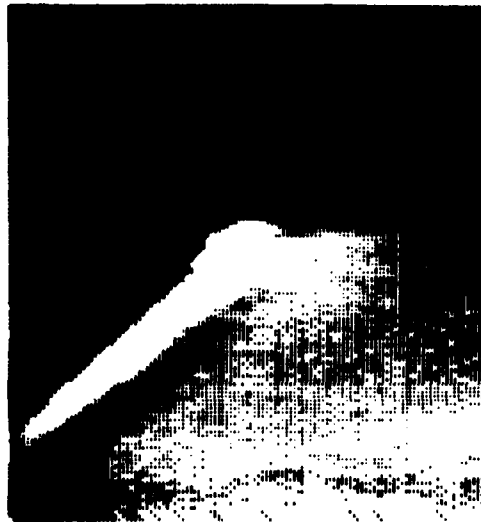
 = regions of high density

Figure 1. Example Center of Mass Vectors for (1) and Edge and (2) a Region of Uniform Intensity.

Suppose we now look at a point (c,d) such that the densities around it are fairly constant. Then the center of mass of a small lamina about it would be close to (c,d) . In this case, a vector from (c,d) to the center of mass would be very small compared to a vector from (a,b) to the center of mass in the previous case.



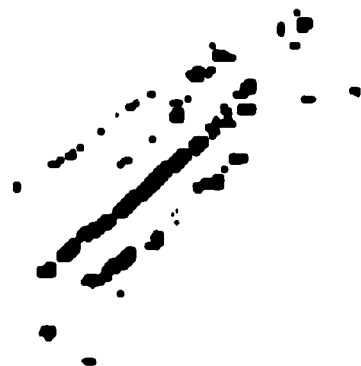
(a) IMAGE OF ROCKET AND PLUME. THE PLUME IS THE LARGE REGION OF HIGHEST INTENSITY.



(b) RAMP AND STEP EDGES FOUND BY USING THE MOMENT OPERATOR.



(c) THE VECTOR FIELD GENERATED BY THE MOMENT OPERATOR.



(d) SECOND ORDER EDGES DETECTED BY USING THE VECTOR FIELD.

Fig. 2

We conclude that one way to transform $f(x,y)$ to $F(x,y)$ such that edges of the original picture lie in the set $F(x,y) > W$ is to replace every $f(x,y)$ by the length of the vector from (x,y) to the center of mass of a small lamina centered about (x,y) . That is, $F(x,y)$ is the magnitude of the vector from (x,y) to the center of gravity of a square lamina centered at (x,y) whose density is given by the picture function $f(x,y)$.

Figure 2(b) is an example of how this method works on a scene (Figure 2(a)) typical of those we study at WSMR.

Once the coordinated (\bar{X}, \bar{Y}) of the center of mass of a lamina about (x,y) are calculated, the direction of the edge (if any) can easily be found. Since (\bar{X}, \bar{Y}) points to where the intensity of the picture is the highest, the direction of the edge is perpendicular to the direction of the vector from (x,y) to \bar{X}, \bar{Y} . If we take $(x,y) = (0,0)$, then the direction of the edge is $\theta = \text{Arctan}(\bar{Y}/\bar{X}) + \pi/2$.

Thus this model gives for each point in the scene a quantity that measures the probability that a point is an edge point and a direction which is the direction of a possible edge through that point.

The model introduced in Section I will not work for roof edges. This is because at the very peak of the roof, exactly where the edge is situated, both \bar{X} and \bar{Y} are equal to zero. In order to detect roof edges we need to take advantage of the direction information, and as Figures 6(a), (b) and (c) show we need to detect the shearing cause by the change in direction of the vector field at the edge points. One way of doing this is by using a tool from the theory of vector fields, namely the rotation of a vector field about a point.

SECTION 2. SECOND ORDER EDGES

After a scene is processed by the moment edge detector, each point is assigned a direction and a magnitude. In effect this specifies a vector at each point of the plan in question; i.e., these vectors define a vector field over the scene. An important tool in the study of vector fields is the rotation of a vector field (see [4] and [5]). To define the rotation of a vector field, suppose a vector of the vector field ϕ at the point (x,y) is given by

$$\phi(x,y) = \{\phi(x,y), \psi(x,y)\}$$

$$\phi(x,y) = \bar{X}(x,y)$$

$$\psi(x,y) = \bar{Y}(x,y)$$

If a curve Γ on the plane (scene) is given in the form

$$\Gamma: x = x(t), y = y(t) \quad a \leq t \leq b$$

then $\phi(t) = \{\phi[x(t), y(t)], \psi[x(t), y(t)]\}$ is defined on the interval $[a, b]$ (see Figure 3).



Figure 3. A Curve Γ and Its Corresponding Vector Field $\phi(t)$

For each $t \in [a, b]$ there is determined an angle, the angle in radians between $\phi(t)$ and $\phi(a)$ measured from $\phi(a)$ to $\phi(t)$. This angle is a many valued function of t . The continuous branch of this function (vanishing for $t = a$) is designated by $\theta(t)$ and called an angular function of the field ϕ on a curve Γ . The rotation of the field ϕ on the curve Γ is defined to be

$$\gamma(\phi, \Gamma) = \frac{1}{2\pi} [\theta(b) - \theta(a)]$$

If Γ is a closed Jordan curve, then the rotation is found by subdividing Γ into two curves (not closed), computing the rotation of each, and adding. In the following, Γ is taken to be a small circle about a point.

We can write the rotation as

$$\gamma = \frac{1}{2\pi} [\theta(b) - \theta(a)] = \frac{1}{2\pi} \int \frac{d\theta(t)}{dt} dt.$$

With $\theta(t) = \text{Arctan } \bar{Y}/\bar{X} + \pi/2$, we make the following observations:

- (1) If $\theta(t) = \text{constant}$, then $\frac{d\theta(t)}{dt} = 0$ and $\gamma = 0$. So $\gamma = 0$ when $x = a$ point on the edge of an object in a scene (see Figure 4).

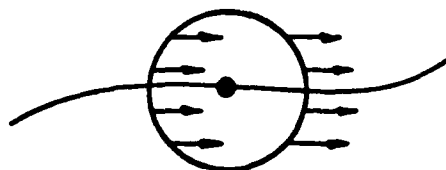


Figure 4. Vector Field at a Step or Ramp Edge Point

(2) If θ is symmetric about x and Γ is a small circle about $x =$ edge point on a roof edge, see Figure 5, then with $\Gamma = \Gamma_1 + \Gamma_2$ (where $\Gamma_1 =$ one half of the circle and $\Gamma_2 =$ the other half)

$$\int_{\Gamma} \frac{d\theta(t)}{dt} dt = \int_{\Gamma_1} d\theta(t) + \int_{\Gamma_2} d\theta(t) = \pi + \pi = 2\pi$$

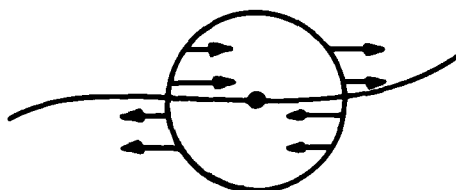


Figure 5. Vector Field at a Roof Edge Point.

An example of how these observations can be used to detect second order edges appears as Figure 6(c) and (d).

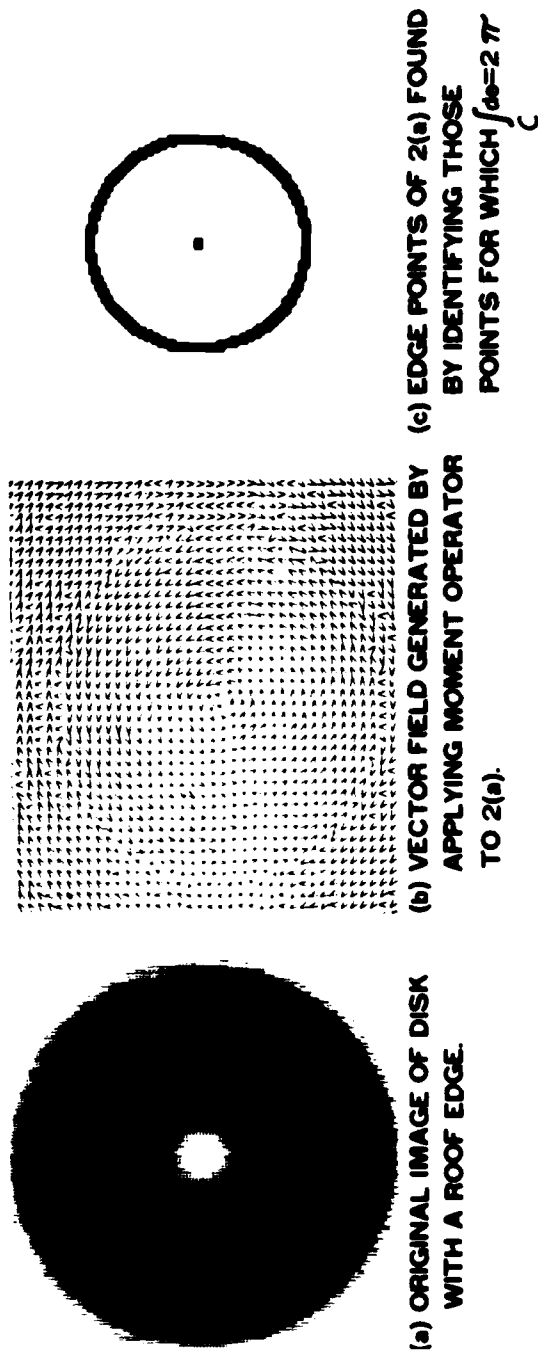


Fig. 6

SECTION 3. ALGORITHMS FOR IMPLEMENTATION

A. Calculation of Moment

Since we are interested in real time applications of these methods we simplify the calculation of \bar{X} and \bar{Y} by setting

$$M = \int_{-h}^h \int_{-k}^k f(x + T, y + u) dt du = 1$$

This can be justified by observing that $M/4hk$ is the average of the intensities over a small neighborhood of (x,y) and so this value can be approximated by the average value of intensities over the entire picture. This would then be just a scale factor and so could be left out.

To calculate the integrals involved we use an integral formula [6] of order $O(h^6)$. The formula for integration is

$$\iint F(x,y) = \sum_{i=1}^9 W_i D_i \text{ with } W_1 = 25/324, W_{21} = 10/81$$

and if we apply this to the integrals for \bar{X} and \bar{Y} and factor out all scale factors we get

$$\bar{Y} = 5 * (D1 - D5) + 4 * (D8 + D2 - D6 - D4)$$

$$\bar{X} = 5 * (D7 - D3) + 4 * (D8 + D6 - D2 - D4)$$

and use $\text{abs}(X)^2 - \text{abs}(Y)^2$ for the associated magnitude. If we sweep a 3×3 window across digitized scene $D7$ can be taken as the upper left hand corner while $D3$ is the lower right hand corner. In this case the direction of a possible edge is equal to

$$\theta = \text{Arctan} \left(\frac{\bar{Y} + \bar{X}}{\bar{Y} - \bar{X}} \right) + \pi/2$$

B. Calculation of the Rotation

The vector field of a roof edge will look like the vector field of Figure 5. So to find roof boundary points we have to find points for which in a neighborhood of such a point $\int_c d\theta = 2\pi$

The smallest region, in the discrete case over which we can take an integral is a 2×2 window. Thus our algorithm sweeps a 2×2 window

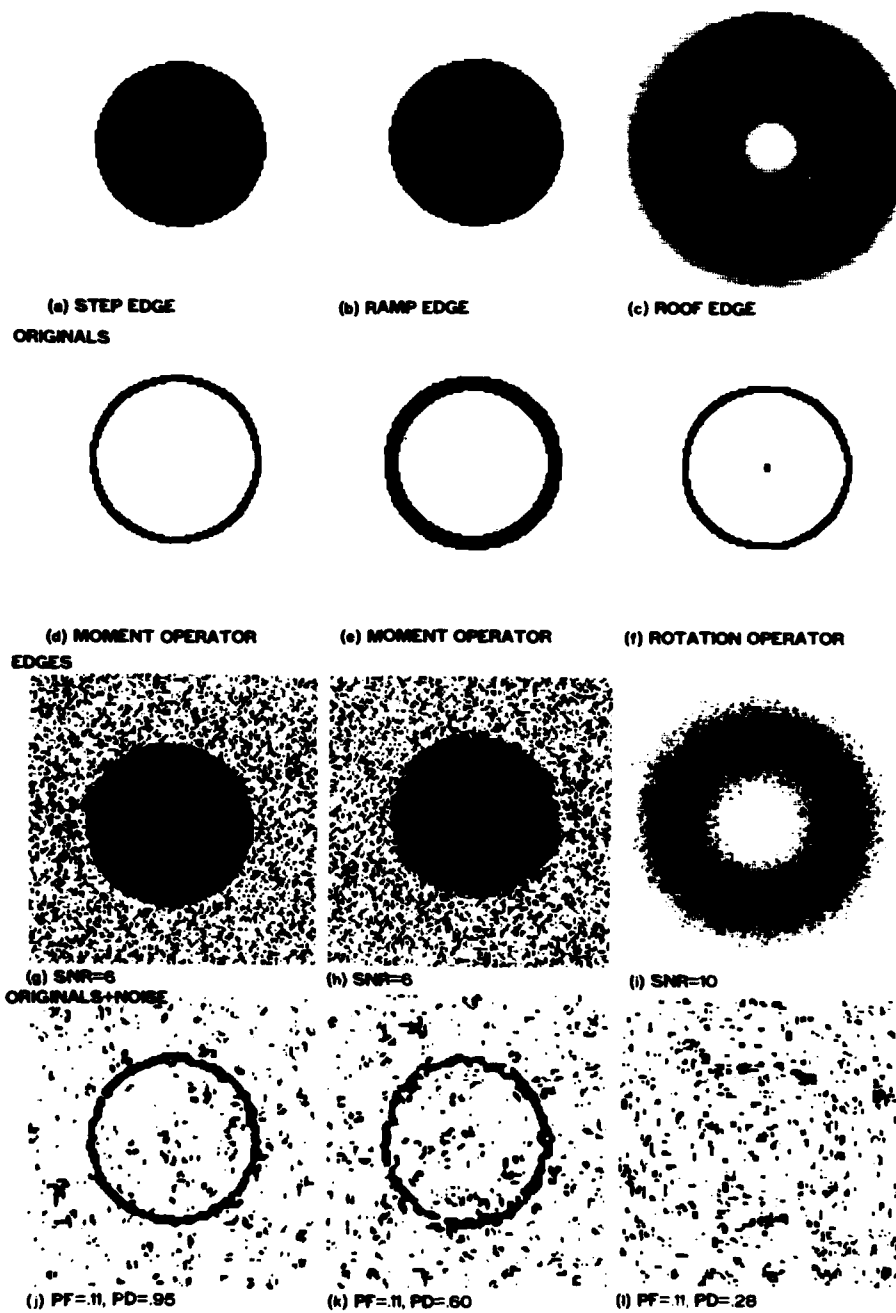
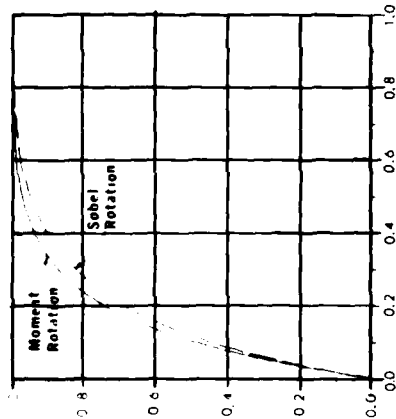


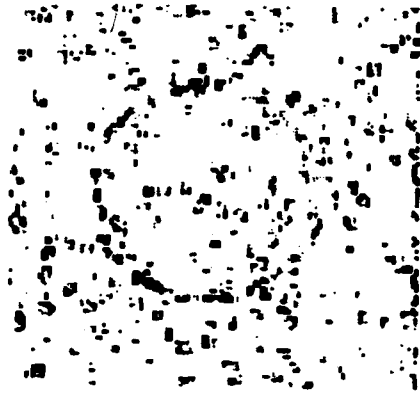
Fig. 7



(a) ROC CURVE FOR ROOF EDGE
AT SN=13. MOMENT EDGE
OPERATOR AND SOBEL EDGE
OPERATOR APPLIED AFTER A
3x3 AVERAGING.



(b) THIS ROOF EDGE WAS
FOUND USING MOMENT
OPERATOR. SNR=13, PF=.10,
PD=.58.



(c) ROOF EDGE WHICH WAS
FOUND USING SOBEL
OPERATOR. SNR=13, PF=.10,
PD=.51.

Fig. 8

464

across a scene and computes the integral $\int_c d\theta$ for each of these windows. If it turns out that this integral is equal to 2π then those 4 points which make up the window are classified as boundary points. To calculate the integral of a 2×2 window we use an approximation

$$\int d\theta = \sum_{\ell=1}^4 \Delta_{\ell} \theta$$

computed by a computer program given in Reference [10].

For the purposes of this experiment the procedure used to generate a file which is the file of detected second order edges in the following:

1. From the original file (scene) two files are generated; one (ACI) contains $\text{SQRT}(\bar{X})^2 + (\bar{Y})^2$; and the other (ANG) the angle of $(\theta, 0 \leq \theta \leq 2555)$ a possible edge.
2. From the ANG and ACI files one new file AAA is created. AAA is created by sweeping a 2×2 window across the ANG file. The rotation is calculated, and if a point is classified as boundary then to the corresponding point of AAA (initialized at zero) is added the average of those elements of ACI that have the same subscripts as those of the 2×2 window being swept across ANG.

Examples of how this method works are Figures 6(c) and 2(d).

SECTION 4. EVALUATION

The methods described above were tested on disks whose edges were step, ramp and roof edges. The step and ramp edges had edge height equal to 16 while the roof edge was constructed by beginning at the center with gray value equal to 100 incrementing by one to gray value equal 132 and then decrementing by one to gray value 100. All files were $128 \times 128 \times 8$.

To test the effectiveness of the different operations considered here we added Gaussian noise of different standard deviation to achieve a given signal to noise ratio and then tested the algorithms (Figure 7).

The SNR ratio was measured in db; that is, we used $\text{SNR} = 10 \log_{10} \left(\frac{16}{\sigma_n} \right)^2$

where σ_m = standard deviation of the noise. For the ramp and step edges we used $\text{SNR} = 4, 5, 6, \dots, 14$ while for the roof edge the

465

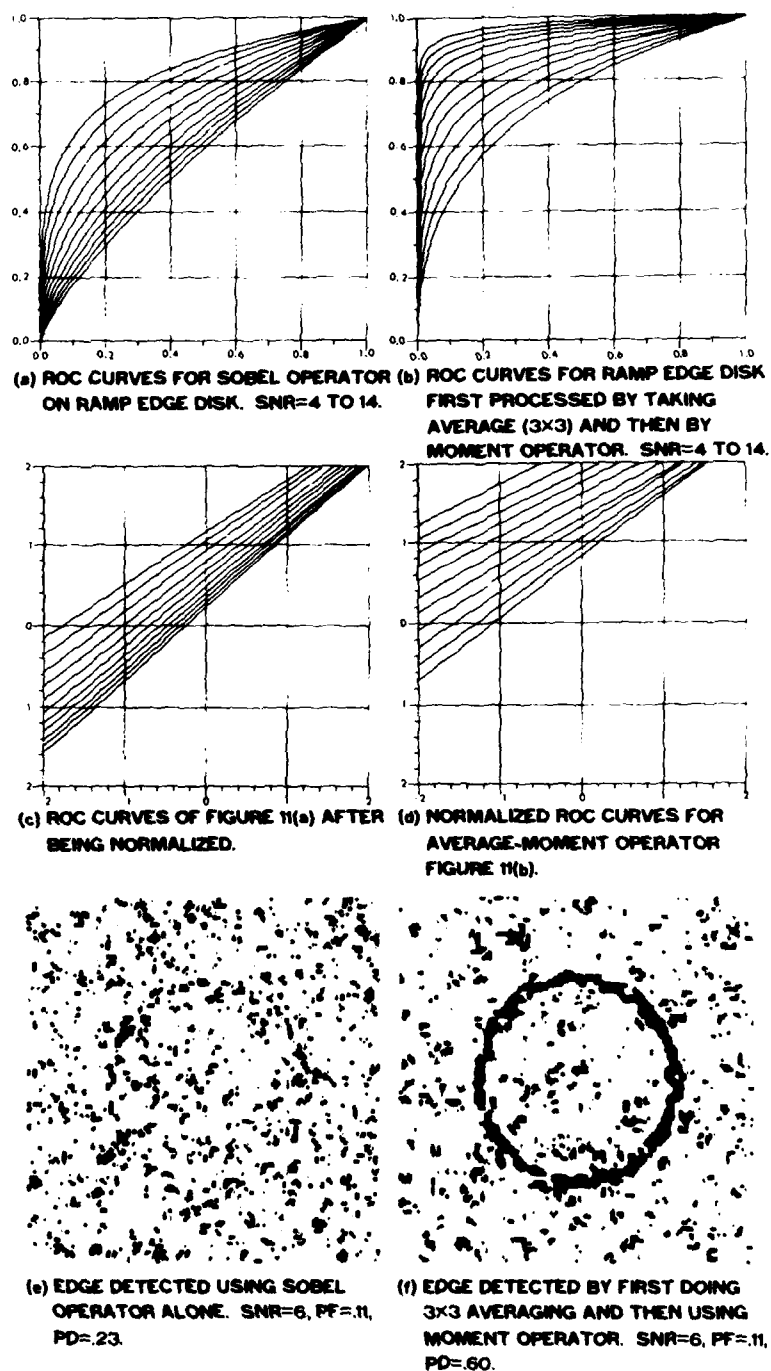


Fig. 9

466

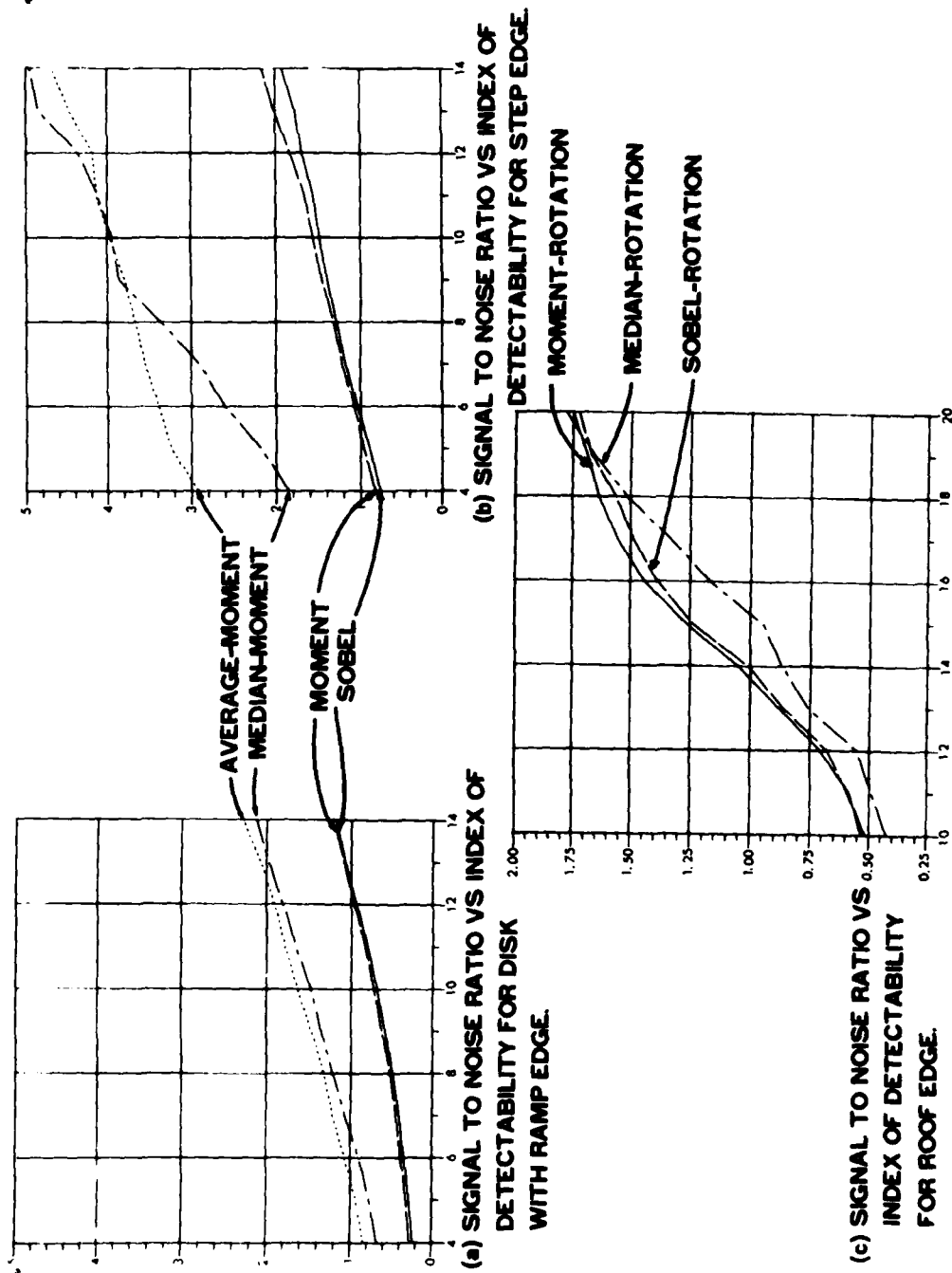


Fig. 10

467

*MACHUCA & GILBERT

signal to noise ratios used were 10, 11, 12, ..., 20. To measure the effectiveness of the different algorithms we graphed PF = the probability of false alarms vs PD = the probability of detection (Figure 9(a) and 9(b), for details see [7]). Figures 8(b) and 8(c) contain examples of processed roof edge disks with SNR = 13. The graphs of PF vs PD (ROC Curves) for the corresponding operators appears in Figure 8(a).

The results for different operators and step, ramp and roof edges appear respectively in Figures 10(a), 10(b), and 10(c). These graphs show that the performance of the moment operator is in all cases better than that of the Sobel operator. A significant improvement is obtained by first applying the average and then the moment operator. When the signal to noise ratio is high the median gives better results than the average, but there is a crossover point at which the average filter gives better results than the median.

REFERENCES

1. A. Rosenfeld and A. Kak, "Digital Picture Processing", Academic Press, New York, NY, 1976
2. B. Lipkin and A. Rosenfeld, "Picture Processing and Psychopictorics", Academic Press, New York, NY, 1970
3. W. Pratt, "Digital Image Processing", John Wiley and Sons, New York, NY, 1978
4. M. Krasnoselsky, A. Perov, P. Zabreiko, "Plane Vector Fields", Academic Press, New York, NY, 1961
5. J. Milnor, "Topology from the Differentiable Viewpoint", University Press of Virginia, Charlottesville, Virginia, 1965
6. A. H. Stroud, "Approximate Calculation of Multiple Integrals", Prentice Hall, Englewood Hills, NJ, 1971
7. I. Abdou, "Quantitative Methods of Edge Detection", Image Processing Institute, University of Southern California, Los Angeles, CA, 1978
8. R. Angus and T. Daniel, "Applying Theory of Signal Detection in Marketing: Product Development and Evaluation", American Journal of Agricultural Economics, Vol 56, No 3, August 1974, (pp 573 - 577)
9. M. Giles, "Grating Detectability: A Method to Evaluate Aberration Effects in Visual Instruments", Optical Engineering, Vol 18, No 1, Jan 79, (pp 33 - 38)
10. R. Machuca and A. Gilbert, "Finding Edges in Noisy Scenes", IEEE Transactions on PAMI, to appear